Low-temperature sintering of silica–boric acid-doped willemite and microwave dielectric properties

Article *in* Japanese Journal of Applied Physics · October 2015

DOI: 10.7567/JJAP.54.10NE03

CITATIONS
3

READS
267

8 authors, including:

Minato Ando
18 PUBLICATIONS **183** CITATIONS
SEE PROFILE

Hitoshi Ohsato
Nagoya Industrial Science Research Institute
317 PUBLICATIONS **10,530** CITATIONS
SEE PROFILE

Yutaka Higashida
CMC Technology Development Co., Ltd.
44 PUBLICATIONS **733** CITATIONS
SEE PROFILE

Akinori Kan
Meijo University
114 PUBLICATIONS **2,300** CITATIONS
SEE PROFILE

Low-temperature sintering of silica–boric acid-doped willemite and microwave dielectric properties

2015 Jpn. J. Appl. Phys. 54 10NE03

(http://iopscience.iop.org/1347-4065/54/10S/10NE03)

Japanese Journal of Applied Physics **54**, 10NE03 (2015) **REGULAR PAPER**
http://dx.doi.org/**10.7567/JJAP.54.10NE03**

Low-temperature sintering of silica–boric acid-doped willemite and microwave dielectric properties

Minato Ando[1], Hitoshi Ohsato[1,3*], Daisuke Igimi[4], Yutaka Higashida[4], Akinori Kan[5], Sadahiko Suzuki[6], Yoshitoyo Yasufuku[7], and Isao Kagomiya[2]

[1]*Functional Materials Laboratory, Nagoya Institute of Technology, Nagoya 466-8555, Japan*
[2]*Department of Material Science and Engineering, Nagoya Institute of Technology, Nagoya 466-8555, Japan*
[3]*Department of Research, Nagoya Industrial Science Research Institute, Nagoya 464-0819, Japan*
[4]*Materials Research and Development Laboratory, Japan Fine Ceramics Center, Nagoya 456-8587, Japan*
[5]*Faculty of Science and Technology, Meijo University, Nagoya 468-8502, Japan*
[6]*Marusu Glaze Co., Ltd., Seto, Aichi 489-0032, Japan*
[7]*Yasufuku Ceramics Co., Ltd., Okazaki, Aichi 444-0838, Japan*
E-mail: ohsato.hitoshi@nitech.ac.jp

Received May 30, 2015; accepted July 6, 2015; published online September 29, 2015

Millimeter-wave wireless communications in a high-level information society have been expanding in terms of high-density data transfer and radar for pre-crash safety systems. For these communications, millimeter-wave dielectrics have been expected for the development of substrates with high quality factor (Qf), low dielectric constant (ε_r), and near-zero temperature coefficient of resonance frequency (TCf). We have been studying several silicates such as forsterite, willemite, diopside, wollastonite, and cordierite/indialite glass ceramics. In this study, the synthesis of willemite and low-temperature-sintered willemite for low temperature co-fired ceramics (LTCC) is examined. The raw materials used for preparing slurries in doctor blade tape casting are also analyzed.

1. Introduction

The Nikkei Electronics (NE) magazine[1)] reported in 2006 in Japan that millimeter-wave wireless communications had begun to spread to public welfare systems. In recent years,[2)] millimeter-wave communications have reached runways to takeoff after many twists and turns. A standard millimeter-wave communication in the 60 GHz zone converges to "IEE802.11ad.", because of its usage in a public welfare apparatus as wireless gigabite (WiGig), which has the highest data communication speed of 7 Gbps, a short communication distance of approximately 10 m, and advanced properties such as security and power control. Non compressed millimeter-wave wireless communications with a high data transfer rate[3)] have been developed to support the individual system interface, which connects PC peripheral devices and a data bus for HDTV, monitors, and projectors. Furthermore, millimeter-wave communication can be applied to radar for pre-crash safety systems.[4)]

Dielectrics for the microwave region[5)] have been researched for a long time, during which some excellent materials[6–11)] have been developed and used for applications. Some of them, such as a complex perovskite,[9)] are used for millimeter-wave wireless communication. Recently, millimeter applications have been developed as stated above. Thus, dielectrics for millimeter-wave communication are expected, which have high quality factor (Q), low dielectric constant (ε_r) and near-zero temperature coefficients of the resonant frequency (TCf).[12,13)] Most of the candidate materials exist in silicates with low ε_r, such as forsterite (Mg_2SiO_4),[14–17)] willemite (Zn_2SiO_4),[18)] and cordierite/indialite ($Mg_2Al_4Si_5O_{18}$),[19,20)] because of reduced rattling in silicate tetrahedra based on covalency.[20–23)] In this study, willemite is applied, which has excellent properties: $Qf =$ 219,000 GHz, $\varepsilon_r = 6.5$, and $TCf = -66$ ppm/°C.[18)] TCf was improved to 1.31 ppm/°C adding a rutile of 11 wt% with other properties, namely $Qf = 118{,}000$ GHz and $\varepsilon_r =$ 9.06.[18,24)]

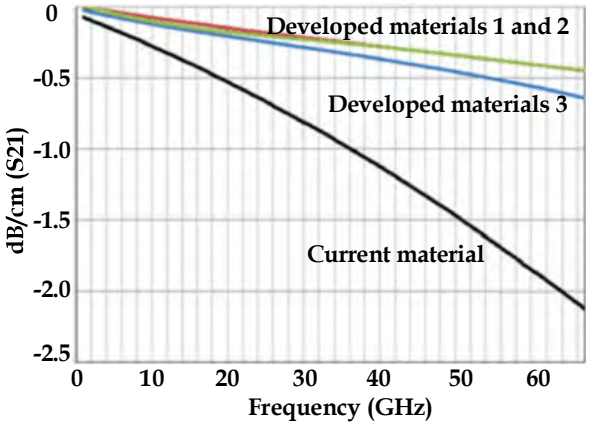

Fig. 1. (Color online) Transmission loss in the microstrip line using high-Q willemite substrate. The loss is 1/10 that in the current substrates.[25,26)]

Fujimoto et al.[25)] reported on the transmission loss in the microstrip line fabricated on the willemite substrate, which is shown in Fig. 1 compared with a current material, as the Supporting Industry project of METI Chubu.[26)] The transmission loss is 0.5 dB/cm (Ag) at 67 GHz, which is 1/10 that in current substrates, indicating that the willemite substrate has the best properties. The willemite substrate and low temperature co-fired ceramic (LTCC) substrates based on willemite[18,24)] will be used for millimeter-wave applications. Convenient mobile equipment is recently expected to be increasingly small, thus, highly integrated circuit such as LTCCs[27–29)] which integrate and build the different components into ceramic began to be applied for miniaturization. Applications in the microwave region have been developed using high-frequency module-compounded duplexers, band pass filters, and low-pass filters, for example. In this region, most LTCC materials such as glass composite materials show a low Q of approximately 200. For the millimeter-wave

Table I. List of low-temperature-sintered willemite for LTCCs.

Sample name	Composition Zn_2SiO_4/SiO_2/as B_2O_3 (wt %)	Sintering agent B_2O_3/H_3BO_3	Sintering agent SiO_2	Solvent	Sintering temperature (°C)
P229	30/55/15	H_3BO_3	SO-E1	Water	700, 725, 750, 775, 800, 900
P231	33/59/8	H_3BO_3	SO-E1	Water	725, 800, 825, 850, 875, 900
P234	33/59/8	H_3BO_3	FQ	Water	800, 825, 850, 875, 900
P215	30/55/15	B_2O_3	SO-E1	Ethanol	825, 850, 875, 900
P216	30/55/15	B_2O_3	SO-E1	Ethanol	825, 850, 875, 900
P217	30/55/15	B_2O_3	SO-E1	Ethanol	825, 850, 875, 900

region, Q is expected to be higher than 500. In this study, a Q higher than 500 calculated as $Qf =$ constant was realized using high-Q willemite.

2. Experimental methods

2.1 Preparation of willemite

ZnO and quartz (SiO_2) were weighed at 500 g in terms of mole ratio: $ZnO : SiO_2 = 2.05 : 1$. These powders were mixed for 48 h in a polyethylene bottle with 2000 ml of distilled water and 350 ml of polyurethane-coated stone balls with a diameter of 10 mm. The obtained slurry was dried for 72 h by fanning at room temperature, and then sieved with a mesh with an opening of 75 μm. The powder placed in an alumina vessel of $150 \times 150 \times 50\,mm^3$ was sintered at 1100 °C for 2 h.

2.2 Preparation of low-temperature-sintered willemite for LTCC

After willemite was synthesized as described in Sect. 2.1, two types of amorphous SiO_2: ADMAFINE SO-E1(>99.9) and HYPRECICA FQ prepared by ADMATECHS and UEXC, respectively, and B_2O_3 and H_3BO_3 were weighed at 35 g in terms of mole ratio, as shown in Table I. Here, SiO_2, B_2O_3, and H_3BO_3 are sintering agents. These powders were mixed for 48 h in a polyethylene bottle with 250 ml of distilled water or ethanol and 100 ml of 8 mm ϕ ZrO_2 balls. During ball milling, 0.3 g each of poly(vinyl butyral) (PVB) and poly(ethylene glycol) (PEG) was added. The obtained slurry was dried for 72 h by fanning at room temperature, and sieved through the mesh with an opening of 75 μm. The obtained dried powders were granulated through the mesh with an opening of 250 μm for the fabrication of pellets. The granulated powder was molded to pellets with 15 mm $\phi \times 10$ mm h using a uniaxial press machine at $300\,kg/cm^2$, and the pellets were subjected to a cold isostatic press (CIP) at $2{,}500\,kg/cm^2$.

2.3 Measurements

Bulk density was obtained from the weight and volume calculated from the size of pellets. Crystalline phases were identified by the X-ray powder diffraction (XRPD) method (Rigaku RAD-C) using θ–2θ scans of Cu Kα radiation. Microstructures were observed by scanning electron microscopy (SEM; JEOL JSM-5200). Microwave dielectric properties of approximately 18 GHz were measured by Hakki and Coleman's method[30,31] in the $TE_{01\delta}$ mode using a network analyzer (Agilent 8720ES). The sample pellets were cylindrical with 10 mm $\phi \times 5$ mm h.

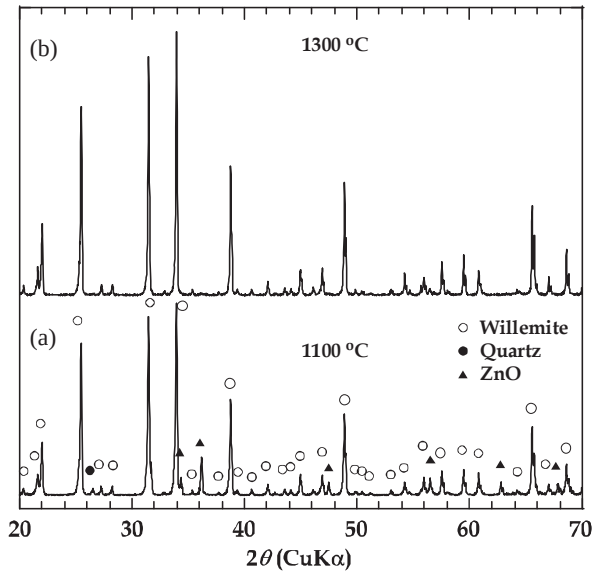

Fig. 2. XRPD patterns of willemite with Zn exceeding 0.05 mol in one formula mass sintered at 1100 °C (a) and resintered at 1300 °C (b). ZnO and quartz in willemite ceramics sintered at 1100 °C reacted to the single phase of willemite at 1300 °C.

3. Results and discussion

3.1 Synthesis of willemite

Figure 2 shows the XRPD patterns of willemite sintered at 1100 °C (a) and resintered at 1300 °C (b). The sample sintered at 1100 °C includes quartz and ZnO. When it was resintered at 1300 °C, it became single-phase willemite. At 1100 °C, as the core of a quartz grain could not react with ZnO, quartz and ZnO remained. At 1300 °C, quartz and ZnO react to form willemite. ZnO is in excess by 0.05 mol because of vaporization. This procedure is based on the results of forsterite sintering reported previously.[16,17]

We determined the optimum sintering temperature of willemite. Willemite powders are synthesized at 1100, 1200, and 1300 °C for 2 h. Ceramics sintered at low temperatures of 825–900 °C were synthesized using willemite at different temperatures and the sintering agents SiO_2 and B_2O_3. Figure 3(a) shows the bulk densities of low-temperature-sintered willemite. Although P215 sintered at 875 °C shows the highest bulk density, the curve of bulk density as a function of sintering temperature is not gentle near 875 °C, showing less margin for control of sintering temperature. On the other hand, having a gentle curve near 860 °C, P216 with willemite synthesized at 1100 °C shows a high bulk density

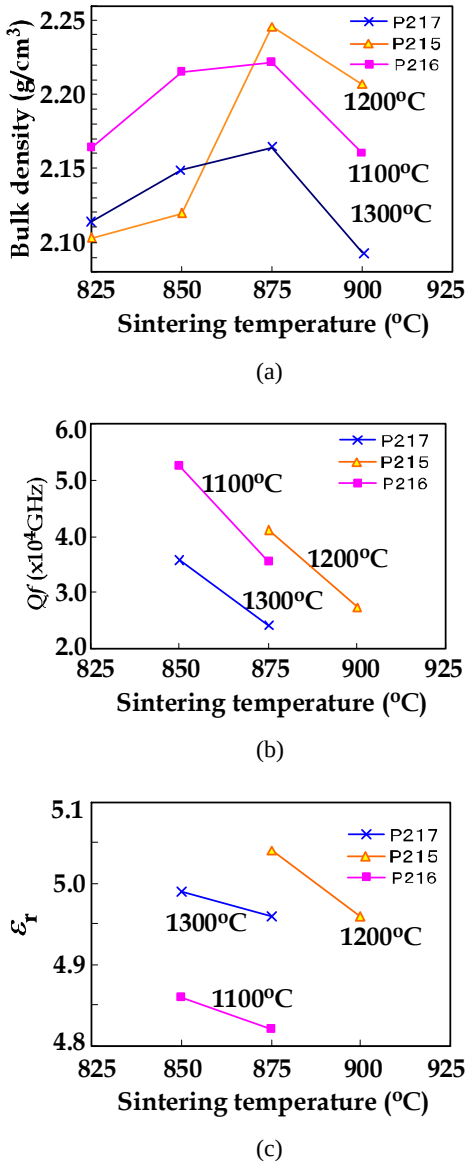

Fig. 3. (Color online) Bulk density (a), Qf (b), and ε_r (c) of low-temperature-sintered ceramics with willemite synthesized at 1000, 1200, and 1300 °C for 2 h.

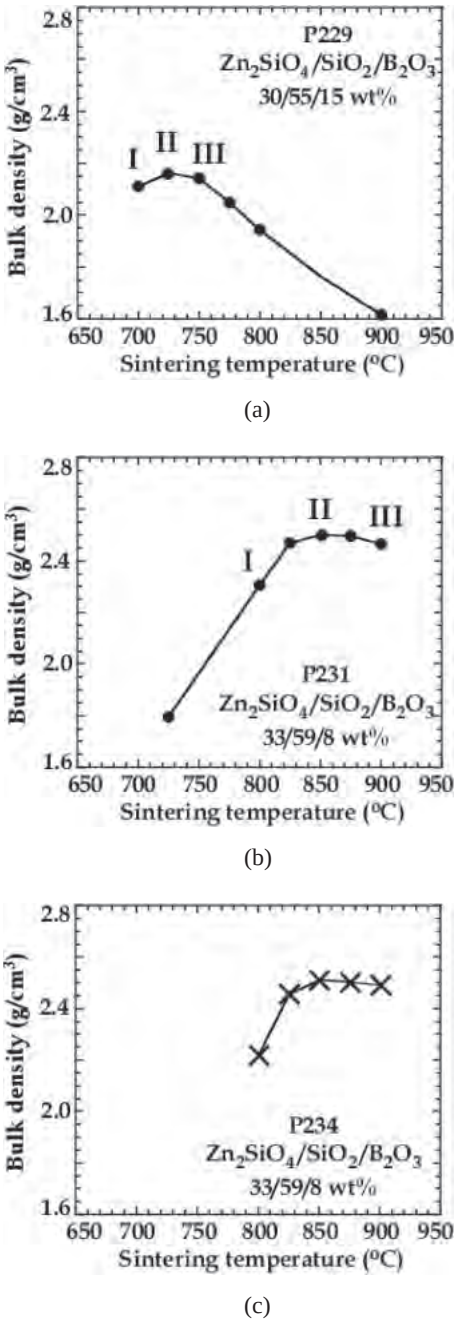

Fig. 4. Bulk density as a function of sintering temperature for P229 (a) with high B_2O_3 content of 15 wt % and P231 (b) and P234 (c) with low B_2O_3 content of 8 wt %. Type of SiO_2: ADMAFINE SO-E1 was used for P229 and P231 and HYPRECICA FQ was used for P234.

and a reasonable margin for control. Figure 3(b) shows the Qf values of the low-temperature-sintered willemite ceramics. Sample P216 with willemite sintered at 1100 °C shows the highest Qf at 850 °C. Therefore, we selected 1100 °C as the optimum sintering temperature for willemite ceramic synthesis. Figure 3(c) shows dielectric constants (ε_r). The selected willemite shows the lowest ε_r, which is expected to be a low dielectric constant for millimeter-wave dielectrics.

3.2 Synthesis of low-temperature-sintered willemite for LTCC

Samples P229 and P231, for which amorphous silica (SiO_2) and boric acid (H_3BO_3) were used as sintering agents, and water as the solvent for ball milling, were sintered at 700 to 900 °C for 2 h, as shown in Table I and Fig. 4. Sample P229 has the highest bulk density at 725 °C and P231 at 850 °C, as shown in Fig. 4. The figure also shows that the bulk density of P229 is lower than that of P231, because P229 has a high content of boric acid. Figures 5 and 6 show, respectively, the XRPD patterns and SEM images of P229 sintered at 700, 725, and 750 °C, denoted as samples I, II, and III, respectively. Most of the peaks on all the XRPD patterns correspond to willemite, and a halo peak at approximately 20 to 30° of 2θ and a unknown phase (◆) are observed. The halo corresponds to the amorphous SiO_2 used as the sintering agent. Sample I in Fig. 5(a) included quartz with the strongest peak (●), which might be crystallized from amorphous SiO_2 at a low temperature of 700 °C. The SEM image in Fig. 6(a) shows a porous sample I as shown by its low bulk density [Fig. 4(a)] because there was no formation of borosilicate glass. Samples II and III in Fig. 6(a) might be including borosilicate glass. A SEM image of sample II

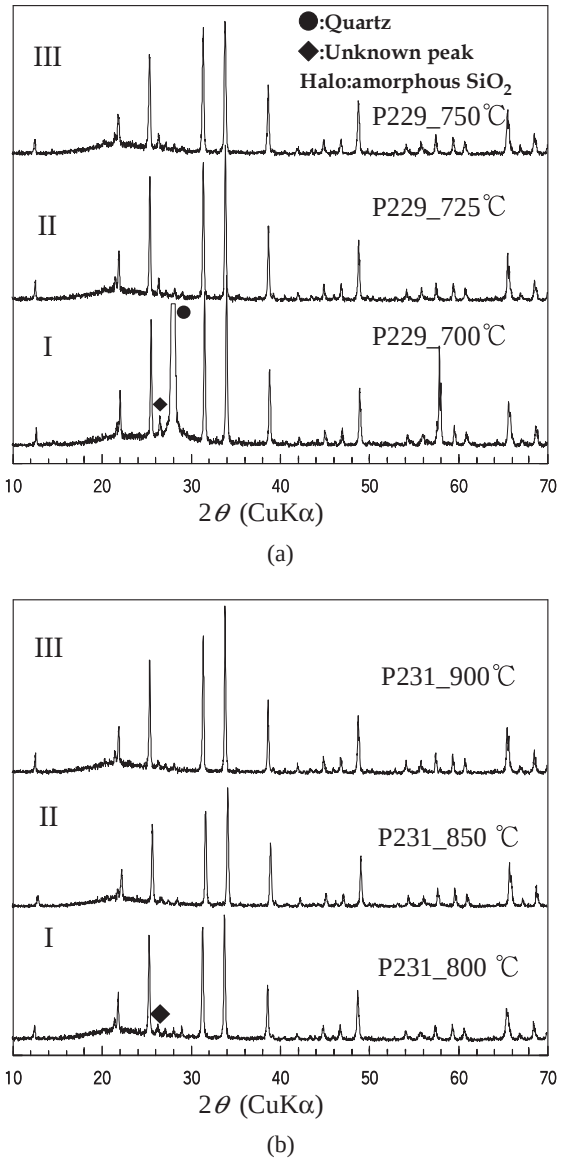

Fig. 5. XRPD patterns of low-temperature-sintered willemite for LTCC. (a) P229 sintered at 700, 725, and 750 °C. (b) P231 sintered at 800, 850, and 900 °C.

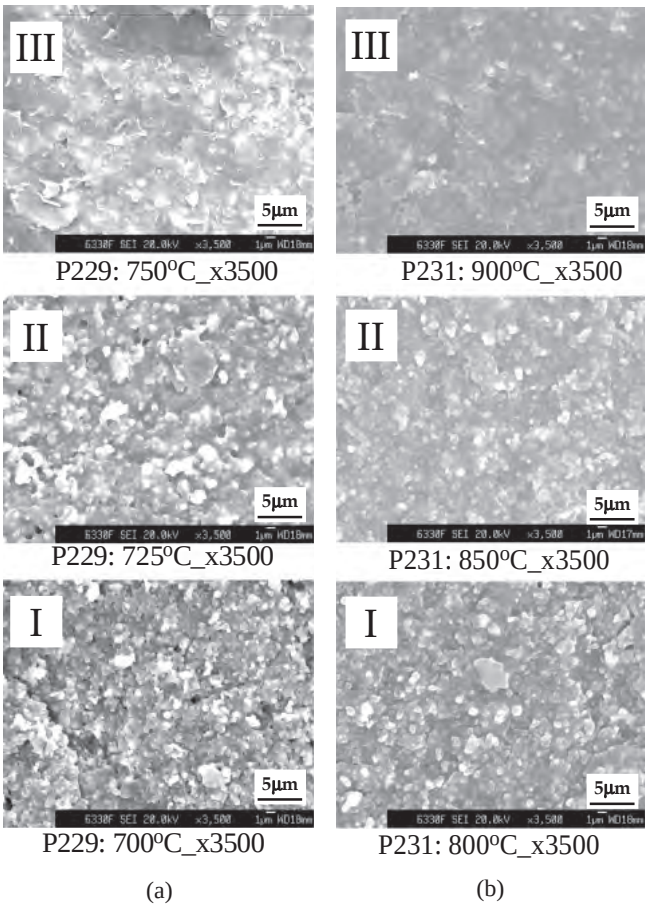

Fig. 6. SEM images of low-temperature-sintered willemite for LTCC. (a) P229 sintered at 700, 725, and 750 °C. (b) P231 sintered at 800, 850, and 900 °C.

shows decreasing porosities; thus the bulk density becomes high. A SEM image of sample III shows a glassy phase, so the bulk density is beginning to decrease.

For sample P231, the XRPD patterns identified the sample as almost willemite, although an unknown phase is observed faintly in sample I in Fig. 5(b). The SEM images also show a similar tendency for P229. Sample P234 was synthesized for confirmation of its microwave dielectric properties, which were almost the same as those of P231 except for the species of SiO_2 used as the sintering agent. The SiO_2 types used for P231 and P234 were ADMAFINE SO-E1 and HYPRECICA FQ, respectively. The bulk densities are shown in Fig. 4(c), which are almost the same as those of P231.

3.3 Microwave dielectric properties

The microwave dielectric properties of P229 and P231 are shown in Table II, whose B raw material was H_3BO_3. P231 samples including a small content (8 wt %) of B_2O_3 show a higher sintering temperature of approximately 850 °C and a higher Qf of $4.04(1) \times 10^4$ GHz than P229, which contains 15 wt % B_2O_3. The Q values of both P229 and P231 are $2.06(1) \times 10^3$ and $2.32(1) \times 10^3$, respectively, which are expected to be higher than 500 at 66 GHz. P229 containing a large content (15 wt %) of B_2O_3 shows a lower ε_r of 4.911(1). This ε_r of less than 5 is desired for millimeter-wave applications. For the comparison of microwave dielectric properties, P234 was also synthesized similarly except for the use of SiO_2 species of FQ as the sintering agent. Its ε_r is almost the same (5.5) as those of the other samples prepared at 850 °C. Its Qf is improved to $4.64(2) \times 10^4$ GHz.

3.4 Which B raw material is better, H_3BO_3 or B_2O_3?

Figure 7 shows bulk density as a function of sintering temperature of P216 on the overlapped Figs. 4(a) and 4(b). The B raw material in P216 is B_2O_3, and in P229 and P231 it is H_3BO_3. Although the composition of P216 and 229 is the same, as shown in Table I, the sintering temperature of P216 is higher than 100 °C. B_2O_3 in P216 reacts with the ethanol solvent as follows:

$$B_2O_3 + 6C_2H_5OH \rightarrow 2B(OC_2H_5)_3\uparrow + 3H_2O.$$

Here, ethyl borate [$B(OC_2H_5)_3$] is produced, which evaporates at room temperature. Therefore, the content (15 wt %) of B_2O_3 is reduced and the sintering temperature is increased to be the same as that of P231 with 8 wt % B_2O_3. However, the bulk density (2.22 g/cm^3) of P216 did not increase, as shown in Fig. 7. The reason is considered as follows: ethyl borate and water generated are decomposed during the sintering,

Table II. Microwave dielectric properties of P229, P231, and P234 measured at approximately 17 GHz.

Sample name (as B_2O_3 wt %)	Sintering temperature (°C)	Frequency f_0 (GHz)	ε_r	$\tan\delta$ ($\times10^{-4}$)	Q ($\times10^3$)	Qf ($\times10^4$ GHz)
P229 (15)	725	18.491870(6)	4.911(1)	4.85(1)	2.06(1)	3.81(1)
P231 (8)	825	17.514948(7)	5.487(1)	5.14(1)	1.94(1)	3.40(1)
	850	17.409574(1)	5.553(1)	4.31(1)	2.32(1)	4.04(1)
	875	17.494679(2)	5.497(1)	4.32(1)	2.31(1)	4.05(1)
P234 (8)	825	17.704814(2)	5.379(1)	3.63(1)	2.76(1)	4.88(2)
	850	17.468357(1)	5.528(1)	3.77(1)	2.65(1)	4.64(2)
	875	17.437035(1)	5.558(2)	3.78(1)	2.64(1)	4.60(1)

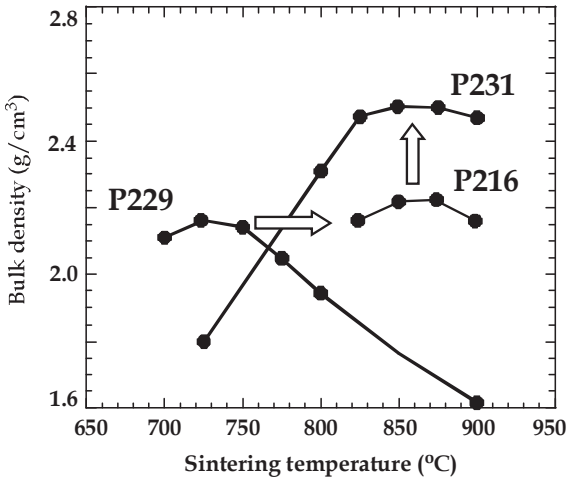

Fig. 7. Bulk density as a function of sintering temperature. As B raw materials, H_3BO_3 was used for P229 and P231, and B_2O_3 for P216.

resulting in a porosity; thus, the bulk density of P216 (2.22 g/cm^3) did not increase to 2.50 g/cm^3.

On the other hand, as H_3BO_3 did not react with water, evaporation of B and the increase in porosity did not occur. In the Supporting Industry Project,[26] originally, we used B_2O_3 as the raw B material for the preparation of the doctor blade slurry, but the slurry was not smooth. The reason is the increased viscosity owing to the reaction between B_2O_3 and ethanol. Therefore, in this study, H_3BO_3 was used instead of B_2O_3 and the solvent used for ball milling was water instead of ethanol. Moreover, H_3BO_3 also did not react with ethanol; thus, the doctor blade solvent could be either ethanol or water.

4. Conclusions

4.1 Synthesis of willemite

SiO_2 and ZnO remain in the willemite ceramic synthesized at 1100 °C, and when it is sintered at 1300 °C, single-phase willemite was obtained. This reaction is explained by core cell formation with the remaining SiO_2 in the core as forsterite, as reported previously.[16,17] The sintering temperature of willemite was optimized for low-temperature-sintering ceramics for LTCCs, which is 1100 °C, as determined from the Qf obtained.

4.2 Synthesis of low-temperature-sintered willemite for LTCCs

Amorphous SiO_2 and H_3BO_3 were used as the sintering agents. The B content of B_2O_3 affected the sintering temperature and bulk density: the sample with 8 wt % B_2O_3 shows a high bulk density of 2.5 g/cm^3 and a sintering temperature of 850 °C, and that with 15 wt % B_2O_3 showed a low bulk density of 2.1 g/cm^3 and a low sintering temperature of 725 °C. The microwave dielectric properties of low-temperature-sintered willemite showed a high Qf of 3.81(1) $\times$ 10^4 GHz and a low dielectric constant of 4.911(1).

4.3 Which B raw material is better, boric–acid or boron oxide?

H_3BO_3 is better than B_2O_3, because B_2O_3 reacts with ethanol to form ethyl borate, which evaporates at room temperature, resulting in pore formation. Moreover, the slurry prepared using B_2O_3 has high viscosity, which makes it difficult to use for doctor blade tape casting. Because H_3BO_3 does not react with ethanol, ethanol could also be used as a solvent.

Acknowledgments

The authors would like to express their thanks to Professor Ken'ichi Kakimoto of NIT and Dr. Kenji Nakahira of JFCC for support in experiments and helpful discussions. Part of this work was supported by the following projects: (1) the Supporting Industry Project of Japan by the Ministry of Economy, Trade and Industry of Japan (METI), (2) MEXT/JSPS KAKENHI (Grant Number 25420721) by the Ministry of Education, Culture, Science and Technology of Japan (MEXT), (3) Adaptable and Seamless Technology Transfer Program (A-step) Japan by MEXT.

1) Nikkei Electronics No. 918 (January 30, 2006).
2) Nikkei Electronics No. 1123 (December 9, 2013).
3) Web [http://keyman.or.jp/3w/prd/78/30001378/].
4) TOYOTA News Release (February 26, 2009).
5) M. T. Sebastian, *Dielectric Materials for Wireless Communication* (Elsevier, Amsterdam, 2008).
6) D. Kolar, Z. Stadler, S. Gaberscek, and D. Suvorov, Ber. Dtsch. Keram. Ges. **55**, 346 (1978).
7) H. Ohsato, T. Ohhashi, S. Nishigaki, T. Okuda, K. Sumiya, and S. Suzuki, Jpn. J. Appl. Phys. **32**, 4323 (1993).
8) H. Ohsato, T. Ohhashi, H. Kato, S. Nishigaki, and T. Okuda, Jpn. J. Appl. Phys. **34**, 187 (1995).
9) E. Koga, H. Moriwake, K. Kakimoto, and H. Ohsato, Jpn. J. Appl. Phys. **45**, 7484 (2006).
10) H. Ohsato, E. Koga, I. Kagomiya, and K. Kakimoto, Key Eng. Mater. **421–422**, 77 (2009).
11) Y. Tohdo, K. Kakimoto, H. Ohsato, H. Yamada, and T. Okawa, J. Eur. Ceram. Soc. **26**, 2039 (2006).
12) H. Ohsato, MRS Proc. **833**, 55 (2005).
13) H. Ohasto, T. Tsunooka, M. Ando, Y. Ohishi, Y. Miyauchi, and K. Kakimoto, J. Korean Ceram. Soc. **40**, 350 (2003).

14) T. Tsunooka, M. Andou, Y. Higashida, H. Sugiura, and H. Ohsato, J. Eur. Ceram. Soc. **23**, 2573 (2003).
15) T. Tsunooka, H. Sugiyama, K. Kakimoto, H. Ohsato, and H. Ogawa, J. Ceram. Soc. Jpn. **112**, S1637 (2004).
16) M. Ando, K. Himura, T. Tsunooka, I. Kagomiya, and H. Ohsato, Jpn. J. Appl. Phys. **46**, 7112 (2007).
17) M. Ando, H. Ohsato, I. Kagomiya, and T. Tsunooka, Jpn. J. Appl. Phys. **47**, 7729 (2008).
18) Y. Guo, H. Ohsato, and K. Kakimoto, J. Eur. Ceram. Soc. **26**, 1827 (2006).
19) H. Ohsato, J.-S. Kim, A-Y. Kim, C.-I. Cheon, and K.-W. Chae, Jpn. J. Appl. Phys. **50**, 09NF01 (2011).
20) H. Ohsato, J.-S. Kim, C.-I. Cheon, and I. Kagomiya, J. Ceram. Soc. Jpn. **121**, 649 (2013).
21) I. Kagomiya, I. Suzuki, and H. Ohsato, Jpn. J. Appl. Phys. **48**, 09KE02 (2009).
22) H. Ohsato, M. Terada, and K. Kawamura, Jpn. J. Appl. Phys. **51**, 09LF02 (2012).
23) H. Ohsato, I. Kagomiya, M. Terada, and K. Kakimoto, J. Eur. Ceram. Soc. **30**, 315 (2010).
24) H. Ohsato and Y. Guo, WO 2006/041093 A1 (20.04.2006).
25) M. Fujimoto, Y. Yasufuku, A. Kan, H. Goto, and S. Hirose, 150th Electronic Ceramic Process Meet., 2015, 26-150-841.
26) Japan Fine Ceramics Center, Report of Supporting Industry Project 2014.
27) M. T. Sebastian and H. Jantunen, Int. Mater. Rev. **53**, 57 (2008).
28) Y. Imanaka, *Multilayered Low Temperature Cofired Ceramics (LTCC) Technology* (Springer, New York, 2005).
29) T. Otagiri, in *Exploitation Technology of Low Temperature Cofired Ceramics (LTCC) in CMC TL 360*, ed. T. Yamamoto (CMC Publishing, Tokyo, 2005) p. 169 [in Japanese].
30) B. W. Hakki and P. D. Coleman, IRE Trans. Microwave Theory Tech. **8**, 402 (1960).
31) Y. Kobayashi and M. Kato, IEEE Trans. Microwave Theory Tech. **33**, 586 (1985).